Observation of Drivers' Behavior at Narrow Roads Using Immersive Car Driving Simulator

Yoshisuke Tateyama[1] Hiroki Yamada[1] Junpei Noyori[1] Yukihiro Mori[1]
Keiichi Yamamoto[1] Tetsuro Ogi[1] Hidekazu Nishimura[1]
Noriyasu Kitamura[1, 2] Harumi Yashiro[2]

[1]Keio University
4-1-1 Hiyoshi, Kohoku,
Yokohama, Kanagawa, Japan
+81-45-564-2498

tateyama@sdm.keio.ac.jp

[2]Tokyo Marine & Nichido Risk Consulting Co., Ltd.
Tokyo, Japan

ABSTRACT
We wish to decrease traffic accidents and want to observe drivers' behaviors to find ways to drive safely. Observations at the real environment include many risks to have needless but critical accidents. Using a car driving simulator, we can observe drivers' behaviors in dangerous situations safely. We constructed an immersive car driving simulator. We conducted an experiment in this immersive environment. The task was that a driver turned a car to the right in the virtual course. The numbers of subjects were one in a real environment and six in a virtual environment. We observed a common behavior of a driver in both environment, two common behaviors of six drivers in virtual environment and two individual variations from six drivers in virtual environment. Our immersive car simulator worked as a simulation of a real driving situation.

Categories and Subject Descriptors
I.3.7 [**Three-Dimensional Graphics and Realism**]: Three-Dimensional Graphics and Realism – *Virtual reality.*

General Terms
Measurement, Design, Experimentation, Human Factors.

Keywords
aging, safe driving, training driving skill, car driving simulator, eye tracking application, CAVE, OpenCABIN library.

1. INTRODUCTION
Observing our driving behavior we can objectively know latent driving problems that we do not know before. For example, how slow my brake pedal depression timing was or whether I failed to pay attention to the objects in right timing. If we fix problems, we will be able to drive more safely. To know our problems in our driving, we can drive at dangerous situations many times. But if we drive at many dangerous situation actually, we will have car accidents actually and suffer heavy losses.

VRCAI 2010, Seoul, South Korea, December 12 – 13, 2010.
© 2010 ACM 978-1-4503-0459-7/10/0012 $10.00

There are many car driving simulators that can simulate many driving situations safely. Even if we have accidents in those simulators, we do not suffer any losses and we can get experiences of dangerous situations.

Many simulators have a small display. We can test some situations in these simulators, but we cannot drive precisely because we cannot recognize whether we are going to hit the wall or not. We cannot recognize relationship between side walls and our car from a normal 2D display. Immersive displays can show objects' size to the viewer, so the driver can guess distances from the car to the walls in an immersive car driving simulator.

We constructed an immersive car driving simulator that was consisted of K-Cave and a car cockpit system with a precise force-feedback function. In this paper, we describe it and experiments.

2. IMMERISVE CAR DRIVING SIMULATOR HARDWARE
We constructed an immersive car driving simulator (Figure 1) that was consisted of K-Cave, a precise force-feedback car cockpit simulator and an eye tracking system. K-Cave consisted of 4 screens, 8 projectors, 5 PCs and a magnetic position sensor system: Ascension Technology Corp.'s Flock of Bird. The car cockpit simulator consisted of a steering wheel that produced precise force-feedback, a brake pedal and a throttle pedal. The steering wheel and the pedals were parts attached in a real car.

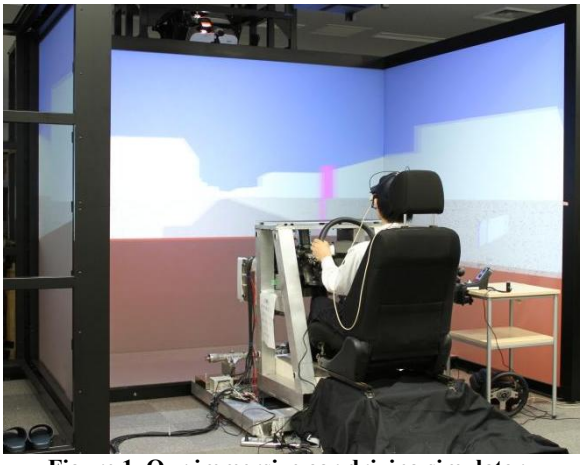

Figure 1. Our immersive car driving simulator.

The details of the hardware and fundamental software used in our immersive car driving simulator are described in [6].

3. MODELING OF VEHICLE

3.1 Vehicle Model

Figure 2 shows a vehicle model to calculate the vehicle motion. The vehicle model is a single track model which consists of two wheels of the front-rear. This model, developed by Segel in 1956 [4], is currently used to describe vehicle dynamic behavior. Nomenclatures using to derive the vehicle model are presented in the Appendix. The parameters of the vehicle model are corresponding of a real vehicle. Equations of motion of lateral and yaw directions of the single track model are given by;

$$m\ddot{y} = F_f + F_r \tag{1}$$

$$I_z\dot{\gamma} = l_f F_f - l_r F_r \tag{2}$$

where $\ddot{y}$ is the lateral acceleration of the vehicle;

$$\ddot{y} = \frac{d}{dt}(V\sin\beta) = \dot{V}\sin\beta + V\cos\beta\cdot\dot{\beta} \tag{3}$$

F_f, F_r is the cornering force generated on the front and rear tires;

$$F_f = -C_f\beta_f = -C_f\left(\tan^{-1}\left(\frac{V\sin\beta + l_f\gamma}{V\cos\beta}\right) - \delta_f\right) \tag{4}$$

$$F_r = -C_r\beta_r = -C_r\tan^{-1}\left(\frac{V\sin\beta - l_r\gamma}{V\cos\beta}\right) \tag{5}$$

By substituting the Eqs. (3) to (5) into the Eqs. (1), (2), we obtain the following;

$$\dot{\beta} = \frac{1}{mV\cos\beta}\left[-C_f\left(\tan^{-1}\left(\frac{V\sin\beta + l_f\gamma}{V\cos\beta}\right) - \delta_f\right) - C_f\tan^{-1}\left(\frac{V\sin\beta - l_r\gamma}{V\cos\beta}\right) - m\dot{V}\sin\beta\right] \tag{6}$$

$$\dot{\gamma} = \frac{1}{I_z}\left[-l_f C_f\left(\tan^{-1}\left(\frac{V\sin\beta + l_f\gamma}{V\cos\beta}\right) - \delta_f\right) + l_r C_r\tan^{-1}\left(\frac{V\sin\beta - l_r\gamma}{V\cos\beta}\right)\right] \tag{7}$$

The vehicle speeds of the X and Y directions and the yaw rate of the vehicle on the global coordinate system as shown in Figure 3 are described as follows;

$$\dot{X} = V_X = V\cos(\varphi + \beta) \tag{8}$$

$$\dot{Y} = V_Y = V\sin(\varphi + \beta) \tag{9}$$

$$\dot{\varphi} = \gamma \tag{10}$$

By integrating the Eqs. (8) to (9), we can obtain the vehicle trajectory;

$$X = \int V\cos(\varphi + \beta)dt \tag{11}$$

$$Y = \int V\sin(\varphi + \beta)dt \tag{12}$$

$$\varphi = \int \gamma dt \tag{13}$$

3.2 Calculation of Vehicle Motion

In order to calculate the vehicle motion based on the driver's maneuver, we compose the Human-in-the-Loop Simulation (HILS) system as shown in Figure 4. The digital signal processor DSP (dSPACE DS1006) is used for the calculation of the vehicle motion by an online. The steering system has been equipped with the steering wheel, an accelerator pedal, and a brake pedal similar to real vehicles. An angle sensor of the steering wheel is installed in the steering wheel. The maximum of the steering wheel angle is $\pm$580 deg. The accelerator pedal has a built-in the sensor that detects the accelerator input u_a by drivers. The brake pedal has the laser type displacement sensor (KEYENCE LB-080) to detect the brake input u_b by drivers. Here, u_a and u_b are detects as the voltage.

The drivers operate the steering wheel, the accelerator pedal, and the brake pedal based on the visual information from the K-Cave. The vehicle motion is calculated using the steering wheel angle θ_h and the accelerator pedal and the brake pedal inputs u_a, u_b which detect from each sensor. The steering wheel angle θ_h is converted into the steering angle of the front tire δ_f by using the steering gear ratio N;

$$\delta_f = \frac{\theta_h}{N} \tag{14}$$

δ_f is input to the single track model. The steady turning radius r_ρ of the vehicle model the is given which depends on the steering wheel angle δ_f and the vehicle speed V as follows;

$$r_\rho = \left(1 - \frac{m}{l^2}\frac{l_f C_f - l_r C_r}{C_f C_r}V^2\right)\frac{lN}{\theta_h} \tag{15}$$

where r_ρ is the distance from the center of the turning radius to the center of gravity of the vehicle. Thus, the turning radius r_ρ considering the steering wheel gear ratio N=16 is 4.117 m at the vehicle speed 5 km/h and the steering wheel angle θ_h=580$\times$(π/180) rad. By using the tread T_r of the center-to-center spacing of right and left wheels, the turning radius at position of the outside tire r_ρ+T_r/2 is 4.9045 m. The vehicle speed V is calculated based on u_a, u_b, which is input to the single track model. Then the vehicle trajectory is calculated from the Eqs. (11) to (13) by using the vehicle state, which is transmitted to the K-Cave system through the Ethernet.

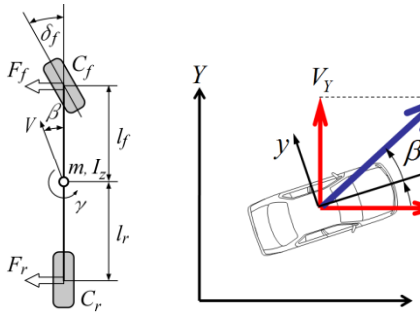

Figure 2. Single track model.

Figure 3. Vehicle trajectory.

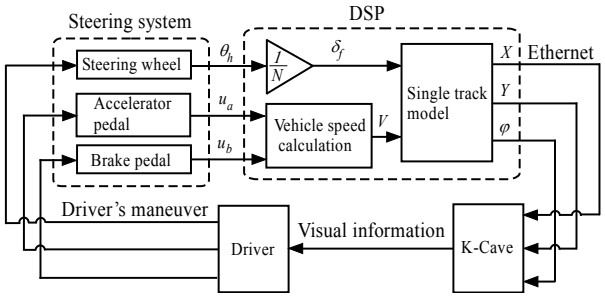

Figure 4. Simulation model of vehicle motion

4. EXPERIMENTAL CONDITIONS

The virtual test course we used in a virtual experiment was designed from the real town: a part of Hiyoshi town in Yokohama city, Kanagawa Prefecture, Japan (Figure 5). The width and the height of our virtual town model were 320 m and 205 m (Figure 6). The width and the length of the virtual car were 1.8 m and 4.95m (Figure 7).

We conducted two experiments observing drivers' behavior. First one was that a driver drove a real car on a real course. The other experiment was that six drivers drove a virtual car in our immersive car driving simulator.

The test driving task was turning right at a crossroad in the virtual Hiyoshi town (Figure 7). The width of the road on which a car was first running was 4.6 m. The width of the road on which the car was running after it turned right at the crossroad was 3.4 m. These dimensions were decided from the real crossroad (Figure 5).

Figure 5. Overview of the real crossroad

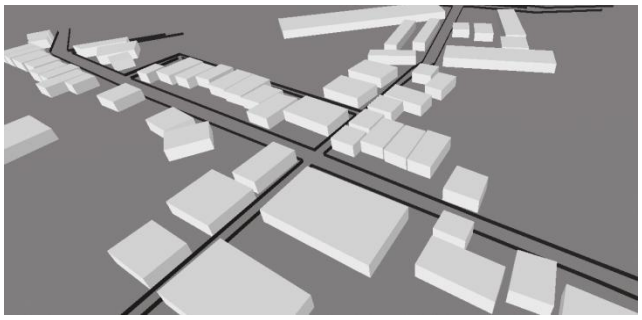

Figure 6. Overview of our test course.

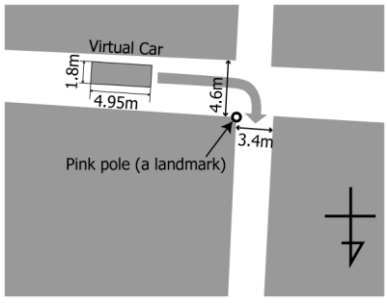

Figure 7. Dimensions of the test course and virtual car. The experimental task was turning right at a crossroad to a relatively narrow road.

Because the second road was very narrow in both real and virtual course, the driver had to pay much attention to right and left side of the car and walls to complete this task.

In the immersive car driving simulator, we could record a wheel steering rotation angle, a degree of depression of pedals, a virtual car position and orientation on a virtual world, a virtual car velocity and the driver's head position and direction. We observed six drivers using the immersive car driving simulator.

5. ANALYSIS OF EXPERIMENTAL RESULTS

We focus on the point of start rotating the steering wheel. In the virtual environment, we can know the precise timing and precise position of start rotating the steering wheel. For the same driver, those points were laid with some trends. Before the discussion about experimental results, we can think the outer edge and inner edge where drivers can take theoretically.

5.1 Theoretical Analysis about Courses

To simplify things, we introduce a hypothesis that the direction of the virtual car is along the broader road before it starts turning right In this theoretical analysis.

As discussed at section 3, the minimal radius of trajectories of this virtual car's center r_ρ is 4.1m. When the car goes along this trajectory, the radius of the outermost point of the car is 3.19m, and the radius of the innermost point of the car is 5.04m.

We can define the outermost trajectory of the center of the car while turning right at this crossroad as depicted in Figure 8. If the car goes out to left, while the car is turning right the rear left corner of the car hits the left wall of the broader road. Also if the timing of the turn becomes late, the front left corner of the car hits to the left wall of the narrow road.

In the same manner, we can define the innermost trajectory of the center of the car while turning right at this crossroad as depicted in Figure 9. If the car goes in to right, while the car is turning right, the right side of the car hits the right wall of the broader road. If the timing of the turn becomes late, the front left corner of the car also hits to the left wall of the narrow road.

Then we can define the "virtual gate" depicted in Figure 10. It shows the limit of going straight along the broader road when the car turn right to the narrower road at this crossroad. When the car go outside of this gate, it cannot turn right without hitting walls.

5.2 Results

Figure 11 and Figure 12 show our experimental results. All points were almost same level horizontally with the virtual gate and naturally before it.

Subject n drove 6 times and positions are within 1m. Subject t and subject y drove 6 or 7 times and positions are within 2m.

Positions of subject k, m and k spread over 3m, but if we can drop first 1 or 2 drives, they were within 3m.

The fact that 6 subjects could drive very precisely in this difficult course can be indicate that our immersive driving simulator could provide a natural car drive environment.

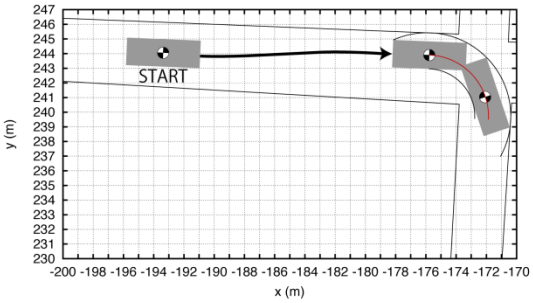

Figure 8. Theoretically outermost success case. The red line shows the trajectory of the center of the virtual car.

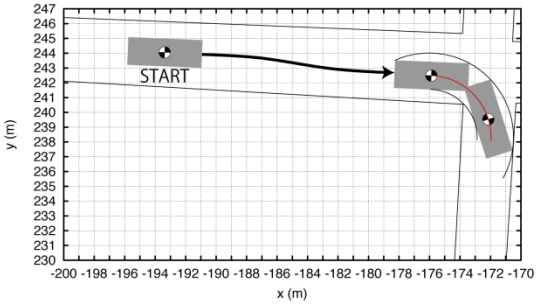

Figure 9. Theoretically innermost success case.

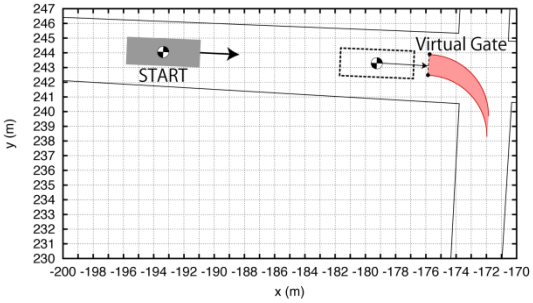

Figure 10. We can define the virtual gate that is the limit of going straight along the road when you turn right to the narrower road.

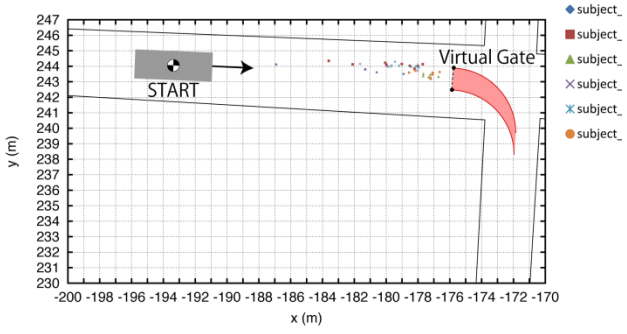

Figure 11. Points of start rotating the steering wheel show trends among subjects.

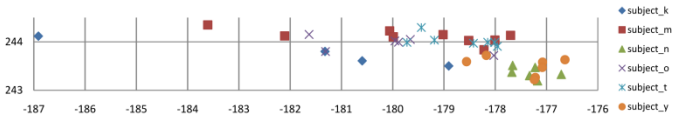

Figure 12. Detail distribution of points of start rotating the steering wheel.

6. CONCLUSIONS

We constructed an immersive car driving simulator with force feedback system in its steering wheel. We conducted an experiment in this immersive driving environment. We observed that 6 subjects could drive very precisely in this difficult course. It can be indicate that our immersive driving simulator could provide a natural car drive environment.

In the virtual environment, we can easily record an angle of the steering wheel, degrees of depressing pedals, the car position, the car orientation, the car velocity and the driver's head angle while it is difficult to know precise information in a real environment.

7. FUTURE WORK

To observe other situations in the virtual environment, we will make the driving course larger and make other situations like some static obstacles. We plan to put moving obstacles on the course.

We want to observe behaviors of elder drivers. But we recognized that this immersive car driving simulator caused so called VR sickness for some people. Some people felt good for over 15 minutes drive in immersive environment but two subjects felt sick within a few minutes. We must investigate this phenomenon and solve this problem.

ACKNOWLEDGMENTS

This research is funded by Tokyo Marine & Nichido Risk Consulting Co., Ltd. Constructing K-Cave was supported by G-COE (Center of Education and Research of Symbiotic, Safe and Secure system Design) program at Keio University.

REFERENCES

[1] Noriyasu Kitamura, "Life Span of Safety Driving," Seiunsya, 2009. (In Japanese)

[2] Cruz-Neira, C., Sandin, D. J., & DeFanti, T. A. "Surround-screen projection-based virtual reality: the design and implementation of the CAVE," In Proceedings of the Computer Graphics Proceedings, pp. 135-142, 1993.

[3] Michitaka Hirose, Tetsuro Ogi, Shohei Ishiwata and Toshio Yamada, "Development and Evaluation of CABIN Immersive Multiscreen Display," Systems and Computers in Japan,scripta Technica,Vol.30, No.1, pp.13-22, 1999.

[4] M. Segel, "Theorical prediction and experimental substantiation of the response of the automobile to steering control," Automobile Div. Inst. Mech. Eng., vol. 7, pp. 310–330, 1956.

[5] Atsushi Arai, Hidekazu Hishimura, Hiroshi Mouri and Masahiro Kunota, "Gain-Scheduled Control of Electric Power Steering," In Proceedings of MoViC 2007, Symposium on Motion Vibration Control, Dynamics, Measurement and Control Division, the Japan Society of Mechanical Engineers, 2007. (In Japanese)

[6] Yoshisuke Tateyama, Tetsuro Ogi, Hidekazu Nishimura, Noriyasu Kitamura, Harumi Yashiro: Development of Immersive Virtual Driving Environment Using OpenCABIN Library, 2009 International Conference on Advanced Information Networking and Applications Workshops (INVITE'2009), pp.550-553, Bradford, 2009.

APPENDIX

Nomenclatures of the vehicle system are presented as the following.

C_f, C_r: Cornering power of front and rear tires

F_f, F_r: Cornering force of front and rear tires

I_z: Yaw inertia moment of vehicle

l: Wheel base ($l = l_f + l_r$)

l_f: Horizontal distance from c.g to front tire

l_r: Horizontal distance from c.g to rear tire

m: Vehicle mass

N: Steering wheel gear ratio

T_r: Track

V_x, V_y: Vehicle velocity on global coordinate system

X-Y: Global coordinate system fixed to the ground

x-y: Local coordinate system fixed to vehicle

β: Slip angle of vehicle

γ: Yaw rate

φ: Yaw angle

C_f=76744 N/rad, C_r=119320 N/rad, I_Z=2243.1 kgm^2, l_f=1.1281 m

l_r=1.4719 m, m=1422 kg, N=16, T_r= 1.575 m